2019-24-0162 Published 09 Sep 2019

Analysis of TWC Characteristics in a Euro6 Gasoline Light Duty Vehicle

Viola Papetti and Panayotis Dimopoulos Eggenschwiler Empa

Vasiliki Emmanouil Exothermia SA

Grigorios Koltsakis Aristotle University Thessaloniki

Citation: Papetti, V., Dimopoulos Eggenschwiler, P., Emmanouil, V., and Koltsakis, G., "Analysis of TWC Characteristics in a Euro6 Gasoline Light Duty Vehicle," SAE Technical Paper 2019-24-0162, 2019, doi:10.4271/2019-24-0162.

Abstract

A Euro6 gasoline light duty vehicle has been tested at the engine dynamometer and the emissions have been analyzed upstream and downstream the Three-Way-Catalyst (TWC) during a WLTC cycle. Catalyst simulations have been used for assessing the processes inside the catalytic converter using a reaction scheme based on 19 brutto reactions (direct oxidation and reduction, selective catalytic reductions with CO, C_3H_6 and H_2, steam reforming, water-gas shift and bulk ceria as well as surface ceria reactions). The reactions have been parameterized in order to best approximate the measurements.

Based on the reactions taken into account, the real vehicle emissions can be predicted with good accuracy. The simulations show that the cycle emissions comprise mainly the cold start contribution as well as discrete emission break-through events during transients. During cold start no reactions are evident in the catalyst before the temperature of the gas entering the catalyst reaches 270°C. Following the light-off, prevailing reactions are direct oxidation as well as surface ceria reactions for CO and THC. NO reduction during cold start is due to reaction with CO as well as due to surface ceria. During warm engine operation, CO break-throughs during transients are mainly due to lack of oxygen following short periods where the engine lambda drops below one and most of surface and bulk CeO_2 has reacted to surface and bulk Ce_2O_3. Moreover in such incidents ceria is reacting with THC forming additional CO. THC break-throughs during transients are mostly simultaneous with CO peaks and are also due to lack of oxygen and depleted CeO_2. NO transient break-throughs occur when engine-out NO sharply increases, and the reactions with CO and ceria are not sufficient.

Further analysis focused in highlighting the effects of variations of Lambda and precious metal content on reaction emissions and mechanisms.

Introduction

Recent legislation concerning real driving emissions are becoming always more and more restrictive and aim to reach zero impact emissions powertrains. If emissions of Euro 6c/d-gasoline vehicles at normal operating temperature are very low, this is not the case during cold start and warming up phase. CO, unburned hydrocarbon (HC) and NO_x emissions are 2-3 orders of magnitude higher during this phase. Moreover, judging by several publications [1, 2, 3], automobile industry is approaching the limits of TWC benchmark effectiveness. For achieving higher performances, further optimization design and of the washcoat require a continuous deeper investigation of TWC system. It is important to build accurate and reliable models of the internal chemical and physical mechanisms. If for steady-state operating conditions, the optimum operating point is well known, which corresponds to the stoichiometric air-to-fuel ratio, and engine management systems are intended to keep the engine operating as close to the stoichiometric ratio as possible, instead, under highly transient conditions such as cold starts, reaction phenomena and consequent optimal design are still under investigation.

The main challenges of TWC modelling are related to the complex interactions between the exhaust species under transient conditions and to the wide variety of washcoat formulations in use. A TWC implies different phenomena: the transport phenomena in the catalyst substrate, the chemistry on the catalytic surface, thus the reactions with respective rate expressions, but also heat and mass transfer and the oxygen storage and release mechanisms. The oxygen mechanisms depend on the redox and temperature under transient operation. In fact, ceria acts as an oxygen buffer and pollutant conversion is also dependent on the state of oxidation of ceria.

Many models proposed in literature about TWC, range from description of detailed mechanism of the catalytic reactions on the surface to purely empirical correlations for the pollutant conversion efficiency [4]. The application of these models for transient exhaust-gas conditions, such as cold starts, usually involves a tradeoff between the chemical background of the model, on one hand, and the computational

load and ease of model parameterization on the other. For instance, models that are based on a detailed kinetics, offer a comprehensive description of the reaction mechanisms including each intermediate step [5], but require high computational effort when attempting to simulate experiments with real exhaust gas. A second approach is instead to model the 'global' chemical reactions, by applying semi-empirical reaction rate expressions, which are usually based on the work of Voltz et al. [6]. This is the case in Oh et al. [7]. To improve model predictions under transient exhaust-gas compositions, several global reaction models have included oxygen storage and release reactions. The operation of the catalytic converter under transient conditions is in fact governed by the oxygen storage and release phenomena, which result from the periodic oxidation and reduction of the ceria found in the catalyst washcoat [8, 9, 10, 11].

Recently, innovative design has been considered: other geometry different from the HC have also been proposed as automotive catalyst substrates. Foams and open cell regular polyhedral structures are able to overcome the limits of laminar flow in HC and require less reacting surface for achieving the same efficiency [12]. Catalysts with foam substrates have already been studied, primarily targeting the simulation of diesel oxidation catalysts and diesel particulate filters [13]. Many studies have been published regarding modelling of pressure drop, mass transfer, and heat transfer in foams [4, 14, 15], and the respective knowledge can be incorporated in models for foam-substrate-based TWC applications. Another innovative technology that requires further modelling efforts is the introduction of an "artificial" supply of energy such as electrical heater or microwave heating source, able to heat up the catalytic converter and reduce cold starts [16].

A great challenge is represented by the validation process of TWC modelling. Chen and Cole [17] validated their model by measurements on a Pt/Rh monolithic converter and modified the kinetic expressions to achieve better agreement with the results of full-scale experiments on an engine. Gottberg et al. [18] conducted extensive trial simulations adjusting adsorption, desorption and reaction rate constants for achieving a satisfactory model validation against real emission data under different dynamic conditions.

This paper presents a complete one-dimensional TWC model for Gasoline Engine developed in the environment of Axisuite, a well established software for after treatment systems [19]. The goal is to offer an exhaustive description of the reaction mechanisms involved in a WLTC cycle of a Euro6 gasoline light duty vehicle within an acceptable computational effort. In fact, Axisuite is able to describe the detailed chemistry phenomena during transient operating conditions. The model is based on 19 brutto reactions and has an oxygen storage submodel for highly transient catalyst operation. The reaction scheme has been tuned in order to best approximate measurements of the vehicle tested at the engine dynamometer. The model is able to capture the performance of the substrate both under cold start and under hot mode conditions. The main mechanisms involving CO, THC and NO_x have been deeply studied both during cold starts and in the warm phase and the effects of several setups, such as the variations of Lambda and precious metal content, have been considered.

Methodology

A Euro6 gasoline light duty vehicle has been tested at the engine dynamometer and the emissions have been analyzed upstream and downstream the Three-Way-Catalyst (TWC) during several real driving cycles. Experiments results have been used to validate and toon the catalytic converter model built in the commercial software Axisuite [19]. Simulations have been used for assessing the processes inside the catalytic converter using a reaction scheme based on 19 brutto reactions (Direct oxidation and reduction, selective catalytic reductions with CO, C_3H_6 and H_2, steam reforming, water-gas shift and bulk ceria as well as surface ceria reactions).

Experiments on the Chassis Dynamometer

Three different real world driving cycles WLTC, FTP75, RDE_Max have been repeated 3 times on the chassis dynamometer of Empa. Although there has been some variability of engine out emissions between the repetitions, the catalyst has smoothed them out. The conversion variability is +- 0.5% in respect to CO, +-0.1% in respect to THC and even 0.05% in respect to NO_x. The vehicle tested is a Euro 6 Gasoline light duty. The driving cycles are representative of real-world traffic situations and are comprising of a transient driving cycle with urban, extra-urban, and motorway parts. During the driving cycles, the exhaust gas temperature and pressure have been measured upstream and downstream of the catalyst. Upstream the catalyst an exhaust probe was mounted and connected via a 5 meter long heated pipe to the exhaust gas analyzer Horiba MEXA 9200DF. Tailpipe emissions have been conducted through a second 5meter heated pipe to a second Horiba MEXA 9200DF. The carbon monoxide (CO), carbon dioxide (CO_2), oxygen (O_2), nitrogen oxide (NO_x), and hydrocarbon (THC) concentrations were measured at 10 Hz sampling rate. It is assumed that the NO_x concentration measured corresponds entirely to nitric oxide (NO), and that the HC concentration measured corresponds entirely to C_3H_6. The ambient temperature was around 20 °C.

Simulations in Axisuite

A Three Way Catalyst (TWC) based on a honeycomb geometry 600 cpsi, 2.5mil with real vehicle dimensions has been simulated with Axicat, an Axisuite application, developed by Exothermia SA. Axisuite. Axicat is the module aimed at the simulation of flow-through, honeycomb catalytic converters and modeling of three way catalysts. The system of differential equations of mass, energy and momentum balances is solved on a 1D mesh. The simulation studies the time range [0,1800]s with a time discretization of 0.5s, while the mesh has space discretization of 1cm. The heat and mass transfer are modelled on the basis of Nusselt and Sherwood number correlations previously published in the literature, the diffusion in the washcoat pores is modelled on the basis of a parallel pores model, and the pressure drop across the substrates is modelled on the basis of correlations adapted from the literature.

FIGURE 1 Axisuite system layout.

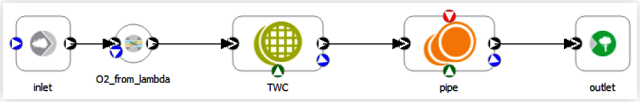

The system layout considered is sketched in Fig. 1: Input measurement data are specified in the module INLET, while in the module TWC the properties of the catalyst substrate have to be set. Results are specified in the Outlet module.

The component called "O2_from_lambda" is able to calculate the inlet O_2 content from the fuel air equivalence ratio λ. The component "pipe" has been used to place the temperature information in the correct location, distant from the outlet of the catalytic converter.

TWC Model

Geometry of the TWC has been specified in terms of length, frontal circular area and overall volume of 2l. Moreover, different models must be introduced:

- The substrate material is cordierite and a built-in library describes the material properties (thermal conductivity, density, thermal capacity, young modulus, etc.) and the diffusion model. Some of the most important model parameters have been reported in Table. 1. Thermal conductivity and thermal capacity have been specified for different temperatures and axisuite calculates the correct value by interpolation or extrapolation. The diffusion mechanisms depend on the substrate pore diameter and on the mean free path of molecules expressed in function of material porosity.
- Concerning the washcoat, the thermal conductivity, the density, the thermal capacity, the diffusion model and the tortuosity are specified. A washcoat loading of 250g/l has been considered. Some of the most important model parameters have been reported in Table. 2. Thermal conductivity is constant, thermal capacity has been specified for different temperatures and axisuite calculates the correct value by interpolation or extrapolation. The diffusion mechanisms depend on the substrate pore diameter and on the mean free path of molecules expressed in function of material porosity.
- Standard canning parameters have been used. In terms of boundary conditions at the periphery, both convection and radiation towards the ambient are taken into account.

TABLE 1 substrate material characteristics.

Property	Values
Thermal conductivity k [W/(m K)]	K(T= 298.15K)=1
	K(T= 1073.15K)=1.2544
	K(T= 1273.15K)=1.88
	K(T= 1473.15K)=2.5
Thermal capacity k [J/(kg K)]	K(T= 300K)=736.13
	K(T= 400)=918.71
	K(T= 600K)=1069.18
	K(T= 1473.15K)=1200
ρ [kg/m^3]	1630
Substrate pore diameter [m]	$13*10^{-6}$
Pore volume fraction [-]	0.35
Substrate tortuosity [-]	3

TABLE 2 washcoat material characteristics.

Property	Values
Thermal conductivity k [W/(m K)]	1.5
Thermal capacity k [J/(kg K)]	K(T= 300K)=736.13
	K(T= 600)=1069.18
	K(T= 900K)=1169
	K(T= 1400K)=1271.87
ρ [kg/m^3]	1630
Substrate pore diameter [m]	$60*10^{-9}$
Pore volume fraction [-]	0.47
Substrate tortuosity [-]	3

Reactions Scheme

The reaction scheme library has been developed starting from a built-in common library present in the environment of Axisuite. 5 reaction groups and in total 19 individual reactions have been considered (listed and numbered for future discussions in Table 3). The groups are: PGM O_2 (indicates the oxidations of CO, HC, NO on PGM sites), PGM NO_x (indicates the reductions of NO_x by CO, HC, H_2 on PGM sites), PGM H_2O (indicates the steam reforming and water-gas shift reactions), bulk ceria reactions (imply the reactions for O_2 storage on Ce sites), surface ceria reactions (are the reactions for O_2 storage on surface Ce sites (surface reactions)). The PGM reactions are modelled as reversible substrate reactions with a Langmuir-Hinshelwood rate expression. The general single reaction equation is described in Eq. 1. The model parameterization (the definition of the pre exponential factors Ai and of the activation energy Ei of each reaction) is performed manually, by analyzing the reaction rates of all the reactions in function of time. The inhibition factors have not been changed. The parameters Ai and Ei of the main reactions of CO, C_3H_6 direct oxidation, of CO and C_3H_6 reactions with surface and bulk ceria, and all the reactions involving NO are modified until an acceptable agreement between experiment and simulation is achieved. Calibration has involved also the choice of the bulk ceria and of the surface ceria storage capacity. In the Langmuir-Hinshelwood rate expressions, inhibition terms G_{Ri} are used in the denominator, to account for the competition of various species to occupy the active catalytic sites. The inhibition terms of oxidation reactions are based on the pioneering work of Voltz et al. on Pt catalysts [10].

Equation 1 chemical reaction equation

$$R_i = \frac{A_i \cdot e^{-\frac{E_i}{RT}} \cdot \prod_s^{1..n_r} c_{p,i,s}}{G_{Ri}}$$

TABLE 3 list of chemical reactions.

Group	Reaction Group	Reactions	NR
I	PGM O_2	$CO + 1/2\ O_2 \rightarrow CO_2$	1
		$H_2 + 1/2\ O_2 \rightarrow H_2O$	2
		$C_3H_6 + 9/2\ O_2 \rightarrow 3\ CO_2 + 3\ H_2O$	3
II	PGM NOx	$C_3H_6 + 9\ NO \rightarrow 3\ CO_2 + 3\ H_2O + 9/2\ N_2$	4
		$CO + NO \rightarrow CO_2 + 1/2\ N_2$	5
		$H_2 + NO \rightarrow H_2O + 1/2\ N_2$	6
III	PGM H_2O	$C_3H_6 + 3\ H_2O \rightarrow 3\ CO + 6\ H_2$	7
		$CO + H_2O \rightarrow CO_2 + H_2$	8
		$CO_2 + H_2 \rightarrow CO + H_2O$	9
IV	Cerium reactions	$bCe_2O_3 + 1/2\ O_2 \rightarrow 2\ bCeO_2$	10
		$bCe_2O_3 + NO \rightarrow 2\ bCeO_2 + 1/2\ N_2$	11
		$2\ bCeO_2 + CO \rightarrow bCe_2O_3 + CO_2$	12
		$2\ bCeO_2 + H_2 \rightarrow bCe_2O_3 + H_2O$	13
		$2\ bCeO_2 + 1/6\ C_3H_6 \rightarrow bCe_2O_3 + 1/2\ CO + 1/2\ H_2O$	14
V	Fast Cerium reactions	$sCe_2O_3 + 1/2\ O_2 \rightarrow 2\ sCeO_2$	15
		$sCe_2O_3 + NO \rightarrow 2\ sCeO_2 + 1/2\ N_2$	16
		$2\ sCeO_2 + CO \rightarrow sCe_2O_3 + CO_2$	17
		$2\ sCeO_2 + H_2 \rightarrow sCe_2O_3 + H_2O$	18
		$2\ sCeO_2 + 1/6\ C_3H_6 \rightarrow sCe_2O_3 + 1/2\ CO + 1/2\ H_2O$	19

Analysis Procedure in Axisuite

Results have been post processed in order to understand the different reaction mechanisms involved overall the WLTC cycle. The focus has been on CO, THC and NO_X peaks. Moreover, the effects of λ and PGM variations have been studied. All tests were repeated with a commercial 2l honeycomb 600 cpsi, 2.5mil monolith. The response of the analyzers often limits the ability to study such rapid transients. A significant distortion is caused by gas mixing inside the exhaust analyzer lines, which tends to dampen peaks in the pollutant concentrations. In this way, highly transient emission peaks appear dampened in the analyzer signal.

Results and Discussion

Comparison between Experiments and Simulations over the WLTC Cycle

The results of the simulation model are compared with experiments in Fig. 3. Cumulative emissions of CO, THC and NO_x downstream the catalyst during the WLTC cycle are plotted in function of time. In Table 4 experimental and simulated cumulative emissions during the overall cycle, but also in the first 300s have been reported. Overall, emissions are very low, thus catalyst efficiency is very high. Moreover, the model

TABLE 4 Cumulative exhaust emissions of CO, THC and NO in [kg], experimental and simulated over a WLTC cycle.

	Experiments	Simulations	Experiments cold starts	Simulations cold start
CO	0.00579	0.00453	0.00079	0.000918
THC	0.000192	0.000162	0.000154	0.000156
NO	0.000249	0.000241	0.000165	0.000157

FIGURE 2 Comparison of measured and simulated temperature time history.

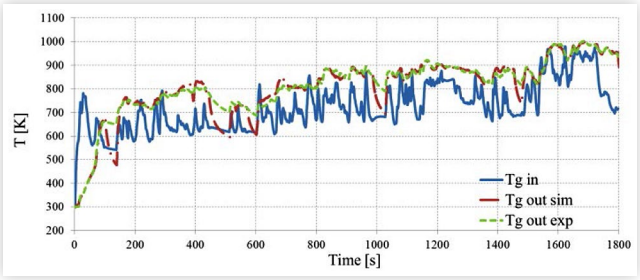

predicts experiments with good accuracy: simulations are able to exactly reproduce NO and THC cumulative emissions, while CO emissions are slightly underestimated by simulations. Even the evolution in time is captured with sufficient accuracy. In particular, THC simulation results overlap with experiments expect for the last 100s of the cycle, where simulations do not reproduce a peak in emissions. Similarly, concerning CO, simulations agree with experiments except in the last part of the cycle where simulations underestimate experimental results. In terms of exhaust temperature, the levels of the outlet temperature are well captured (Fig. 2) by the simulations, which suggest that the reaction enthalpies are correctly computed. However, there are some limited temperature variations that simulations show and which are not seen in experiments. These can be related to the nature of the experimental setup which consists in relatively long pipe connections from the measuring locations to the exhaust gas analyzers and the different responses of the different measurement devices. These inaccuracies are encountered only in temperatures well above light-off temperature; therefore they do not affect the accuracy of simulations of pollutant emissions [4].

It is also important to underline that:

- Measured THC has been modelled in simulations as C_3H_6.
- For tuning the model, only results from entire complex real driving cycles have been available. Modal analysis providing exhaust gas composition averaged over distinct driving operation modes does not usually suffice for modeling purposes. Since a significant portion of the total tailpipe emissions in such systems arise from highly transient short duration modes (idling, acceleration, constant speed, deceleration), it is critical to have time resolved input data at a minimum of 10Hz. For an improved tuning process, specific and controlled

FIGURE 3 Comparison of measured and simulated cumulative exhaust emissions of CO (a), THC (b), and NO (c) in time.

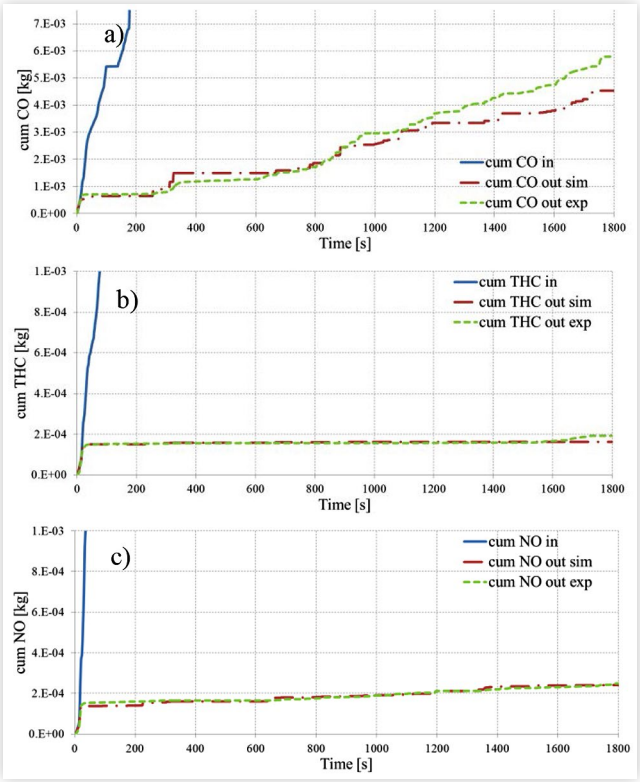

FIGURE 4 Chemical reaction mechanisms related to a discrete CO emission peak around 668s. In Fig. 4c in the legend the numbers correspond to reactions, which are specified in Table 3.

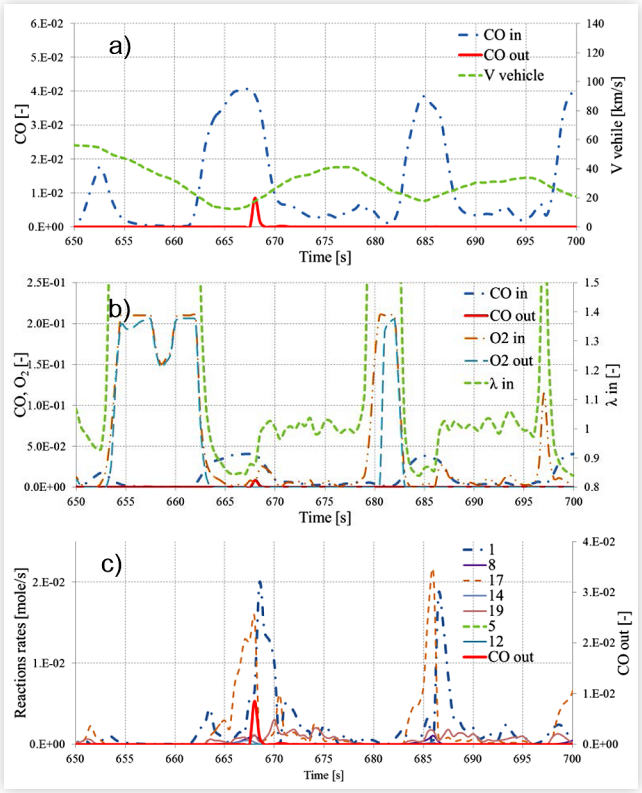

experiments would have been required, if possible with only one reacting species.

- The experiment technique with the classical exhaust gas analyzers (FID, CLD, NDIR) is not able to reproduce abrupt changes in operating conditions with high accuracy. The results are rather to be seen as averaged behavior description. The averaged behavior is due to the inertia along the pipe from the sampling point to the analyzer. More advanced techniques, such as fast FID would allow more precise measurements of HC.
- As a consequence of the averaged nature of the measurement system, the main differences between experiments and simulations are evident during cold starts.

Fig. 3 clearly shows that the cycle emissions comprise mainly cold start contribution and partly discrete emission break-through events during transients. This is evident especially in simulations, less in experiments where the results are smoothed by the measurement setup. In the next sections the chemical mechanisms pertinent for each event type are analyzed in detail.

CO Emission Peaks during the Warm Part of the WLTC Cycle

Several discrete increases in CO emissions are evident in Fig. 3, after the first 300s where the catalytic converter is in a warm phase. These discrete increases are all characterized by a similar chemical mechanism. For instance, Fig. 4 describes CO peak happening around 668s as seen by the trend of CO_{out}. CO emission outlet (CO_{out}) and inlet (CO_{in}) of the catalyst are plotted in Fig. 4a with the velocity profile of the vehicle (V vehicle) and in Fig. 4b with the fuel air equivalence ratio (λ), and with the oxygen concentrations both entering (O_{2in}) and exiting (O_{2out}) the catalyst. All CO relevant reaction rates are plotted in Fig. 4c.

All CO peaks in the warm cycle part occur after a vehicle deceleration (low vehicle velocity), with corresponding fuel cut off phase. In this condition, the catalytic converter is filled with O_2 (λ>>1) and direct oxidation is promoted. Thereafter and during the reacceleration, there is a period characterized by a rich mixture (λ>1) with lack of O_2. The insufficient O_2 is evident in Fig. 4b from O_{2out} profile. CO peak stops when direct oxidation starts again.

The main mechanisms for the CO depletion are direct CO oxidation, CO reaction with H_2O, NO reduction, and surface and bulk ceria reactions. As long as enough oxygen is available, CO conversion is mainly due to direct oxidation and surface ceria reactions. As soon as there is lack of oxygen, the main conversion mechanism for CO become the surface Ce reactions, till all surface CeO_2 cites are depleted. Immediately thereafter, the CO peak occurs. However in parallel, some (but minor) CO is formed as products of the reactions of bulk and surface ceria with C_3H_6.

THC Emission Peaks during Warm Phase

THC emissions behave similar to CO and the peaks of both species are almost synchronized. Fig. 5 analyzes the THC peak that happens contemporaneously to the CO peak described in Fig. 4 (around 670s). All THC peaks in the warm cycle phase have the same reaction mechanism. Fig. 5a describes the THC_{in} and THC_{out} trend, as well as the fuel air equivalence ratio, λ, while Fig. 5b reports all THC relevant reaction rates.

In the same way as with CO, THC peaks occur after a reacceleration period characterized by a rich mixture (λ>1) coming from the engine, with lack of O_2. CeO_2 both surface and bulk react with C_3H_6 till they are depleted. Immediately after, the THC peak occurs. THC peak diminishes thanks to reactions with surface ceria.

On the whole the main reactions occurring are direct oxidation, the ones with surface and bulk ceria, but also with water.

NO Emission Peaks during Warm Phase of the WLTC Cycle

NO emissions mechanism differs from the one of CO and THC: Fig. 6 describes the behavior characteristic of NO peak during the warm phase of the cycle. NO peaks are not synchronized with CO and THC emissions. NO concentrations entering (NO_{in}) and exiting (NO_{out}) the catalyst are plotted in addition to the vehicle velocity profile in Fig. 6a and in addition to λin in Fig. 6b. Fig. 6c describes the rates of the most important reactions involved. The main mechanisms for the NO depletion are reduction with CO and surface ceria reactions, but also with H_2. NO peak occurs after a lean phase:

FIGURE 5 Chemical reaction mechanisms related to a discrete THC emission peak around 668s.

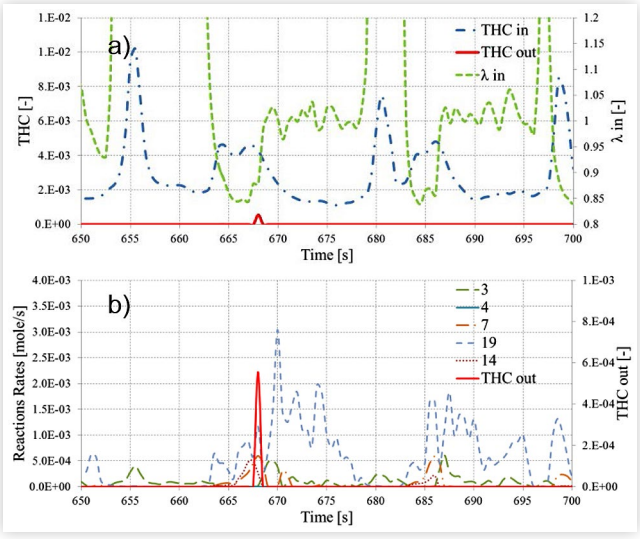

FIGURE 6 Chemical reaction mechanisms related to a discrete NO emission peak around 610s.

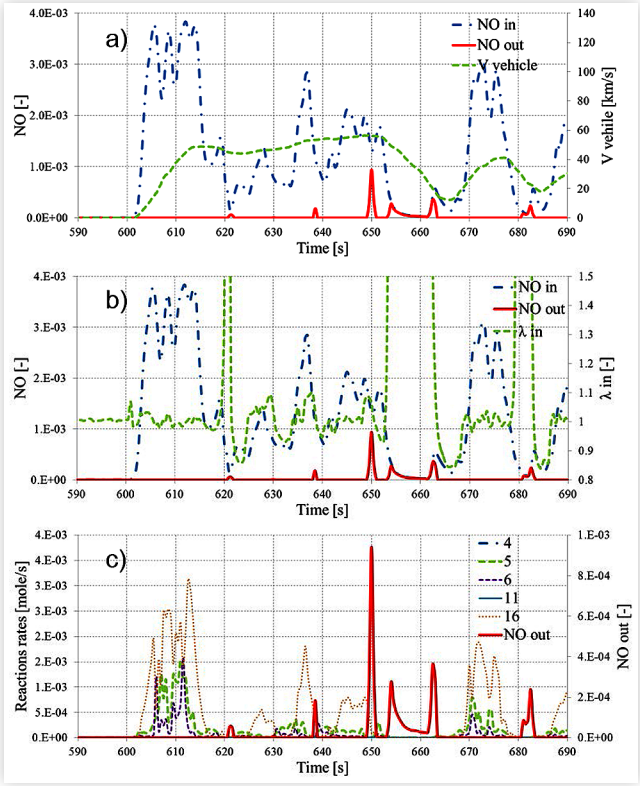

FIGURE 7 Time history of relevant species involved in NO emission peak around 610s: surface Ce_2O_3, H_{2in}, CO_{in} and NO_{out}.

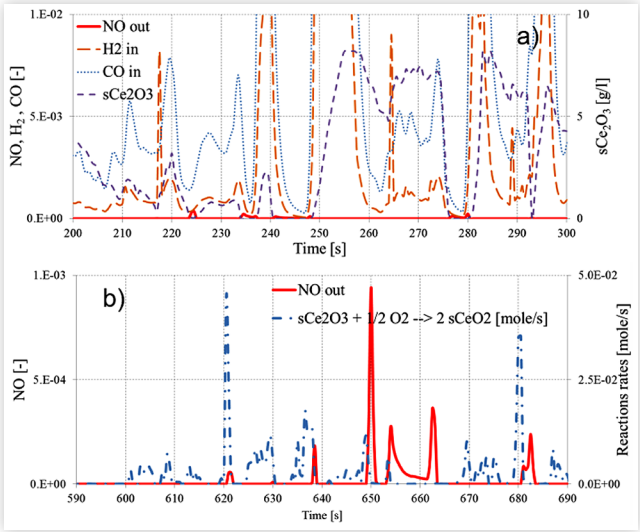

the engine-out NO (NO_{in} for the TWC) is high but there is not enough CO, H_{2in} and sCe_2O_3 for reactions to happen. This is clear also from Fig. 7 where CO_{in}, H_{2in} and sCe_2O_3 (a) and the reaction rate of sCe_2O_3 converted in CeO_2 (b) are reported. During NO peaks, CO_{in}, H_{2in} are very low and sCe_2O_3 is depleted.

Chemical Reactions during Cold Starts

Most of the emissions along the entire WLTC cycle occur during cold starts. According to simulation results, 20.3% of CO, 96.4% of THC and 64.8% of NO emissions happen in the first 300s of the WLTC cycle (300s taken as time limit for cold start period). Fig. 8 a,b and c report cumulative emissions time histories for CO, THC and NO with temperature respectively. In Fig. 8d the instantaneous emissions of the same species for the first 300s are reported. During cold starts no reactions are evident in the catalytic converter before the temperature of the entering gas reaches 270°C (this occurs around time=20s). Moreover, in Fig. 8d it is evident that the predicted emission peaks especially of the species CO and THC are almost synchronized in time. In the following subparagraphs the reaction mechanisms of CO, THC and NO during cold starts are analyzed.

FIGURE 8 Cold starts cumulative and instantaneous emissions in the first 300s of a WLTC cycle. The exhaust gas temperature at the converter inlet is also plotted in the graph.

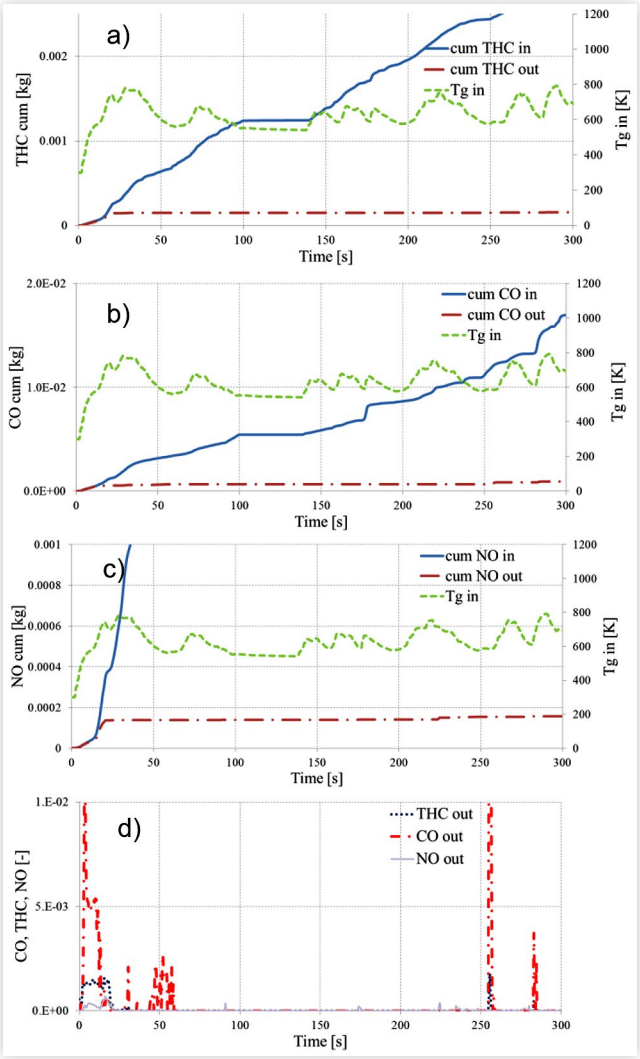

CO Cold Start Emissions

During the first 20s no reactions take place and the first CO peak is due to low temperature, thus catalyst inactivity. Instead, all the other CO peaks shown in Fig. 8c have a similar mechanism to the one described in Paragraph "CO emission peaks during the warm part of the WLTC cycle". Fig. 9b studies CO peaks during cold starts at 250s and 282s. In Fig. 9b the reaction rates history is reported with the addition of the vehicle velocity profile. It is evident that the most important reaction mechanisms for CO depletion are surface ceria reactions and direct oxidation. Moreover, production of CO is also due to C_3H_6 reactions with surface ceria. In Fig. 9c CO_{in} and CO_{out} are plotted with O_{2in}, O_{2out} and sCe_2O_3. The peak occurring at instant 255s happens after a deceleration, at the beginning of a phase of engine cutoff. This is a rich mixture phase, when CO_{in} exiting the engine is high and O_{2in} is low. Co_{in} coming from the engine is high, the O_2 is depleted and no direct oxidations occur any more, while sCe_2O_3 reaction occurs but is not able to reduce CO entirely. The smaller peaks occurring at instant 283s are also related to high CO_{in}. In this case, both reactions happen, all O_2 is depleted and sCe_2O_3 not completely. The same considerations can be applied to THC peaks during cold starts. Exactly at instant 255s a THC peaks occur and the reactions mechanism is analogous to the one described in Fig. 5.

FIGURE 9 Cold starts chemical reaction mechanisms related to CO emission peaks in the first 300s (a). Detailed analysis of CO peak happening in the time span t=[255, 283]s (b, c).

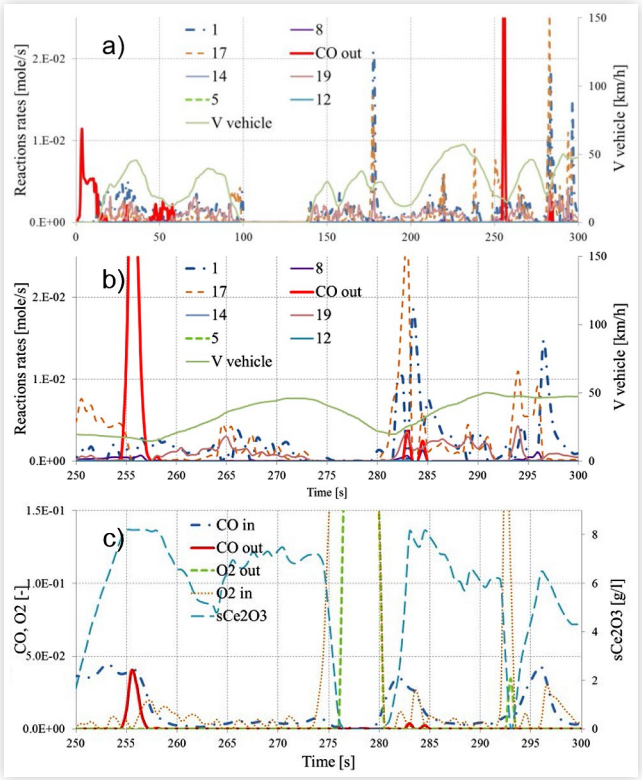

NO Cold Start Emissions

Fig. 10 describes NO reaction mechanisms during cold starts. Plotted are instantaneous concentration before (NO_{in}), and after (NO_{out}) the catalyst with velocity of the vehicle (V vehicle) (Fig. 10a) and with the fuel air equivalence ratio, λ (Fig. 10b). Moreover, all relevant reaction rates (Fig. 10c) and species involved (Fig. 10d) are reported. The kinetic expressions for NO reduction present greater difficulties due to the high redox sensitivity and the complex dependence on CO availability. First of all, in Fig. 8d it is evident that NO emissions characterizes the first 20s and are due to temperature insufficiency, while after that the emissions are very low. NO emissions are not precisely synchronized with CO and THC mechanisms. In Fig. 10 it is decided to analyze the time range [200,300]s, where some very small NO emissions occur. NO emissions happen during deceleration and thus lean periods. The main mechanisms for NO depletion remain the reactions with CO, H_2 and with surface ceria, as it happens during warm phases. Emissions happen when sCe_2O_3, CO and H_2 are not enough for the total reduction of NO.

FIGURE 10 Cold starts chemical reaction mechanisms related to NO emissions in the time range [200,300]s.

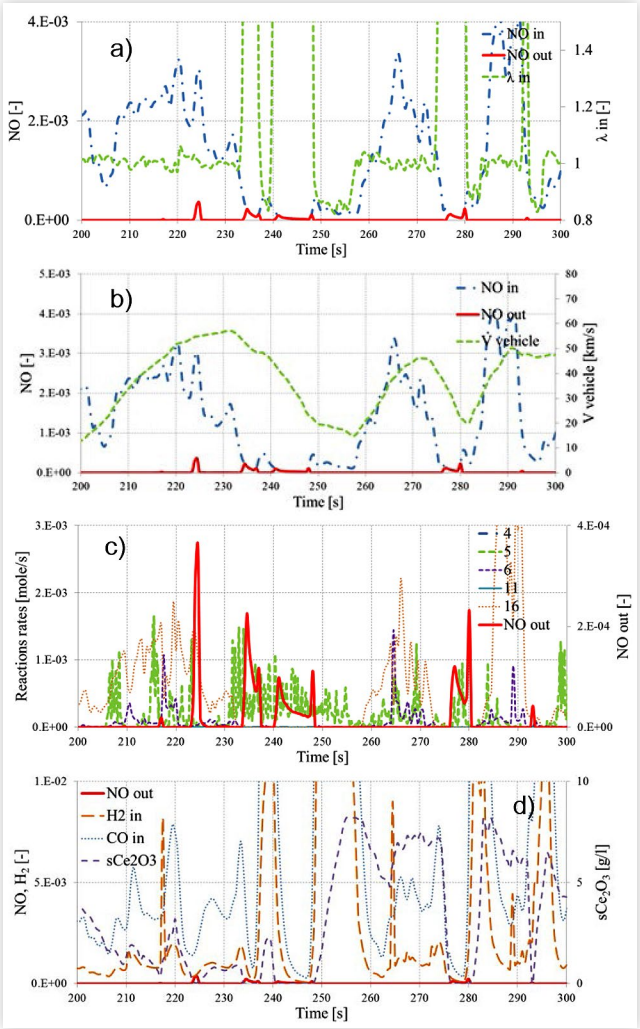

Analysis of the Sensitivity of Result Emissions to λ Variation

The analysis conducted in the previous paragraphs has shown the importance of O_2 in the reactions mechanisms. Here it is decided to investigate the effects of a richer and leaner mixture entering the catalytic converter. Precisely, starting from the base case, λ has been increased and decreased both by 2.5% and 5%. In Fig. 11 the temperature differences across the catalytic converter have been plotted for the different cases. Temperature trends remain similar. Cumulative emissions results are reported in Fig. 12 for CO (a), THC (b) and NO (c) respectively. The cumulative efficiencies, both over the entire WLTC cycle and only in the first 300s, have been also reported in Table 5. The impact of λ is relevant on emissions. On the whole, it is possible to notice that:

- Higher the λ, thus higher O_{2in}, implies higher CO and THC reduction, but also lower NO reduction.
- The effects of λ are stronger on CO, than on THC conversions.
- Considering CO and THC emissions over the entire cycle, the effect of lower λ is higher in percentage than the effect of a proportional higherλ. For example, a reduction of a factor of 1.05 in λ causes a reduction of more than 60% in CO conversion efficiency and of 4% in THC conversion efficiency, while an increase of a factor of 1.05 allows an increase of 2.86% in CO conversion efficiency and of 0.28% in THC conversion efficiency.
- Considering the entire cycle, the effect of lower λ on NO emissions is less evident than the effect of a proportional

TABLE 5 Cumulative efficiency of CO, THC and NO with different λ both on the overall WLTC cycle and on the first 300s.

	η_{CO} [%]	η_{THC} [%]	η_{NO} [%]	η_{COcc} [%]	η_{THCcc} [%]	η_{NOcc} [%]
BASE	96.9	99.3	99.7	94.6	95.1	98.0
λ*1.025	99.5	99.5	715	97.3	96.4	69.8
λ/1.025	58.9	97.8	99.8	63.8	87.6	98.4
λ*1.05	99.7	99.5	51.1	97.7	96.8	44.2
λ/1.05	33.0	95.2	99.8	35.7	77.4	98.7

FIGURE 11 Temperature time history for varying λ.

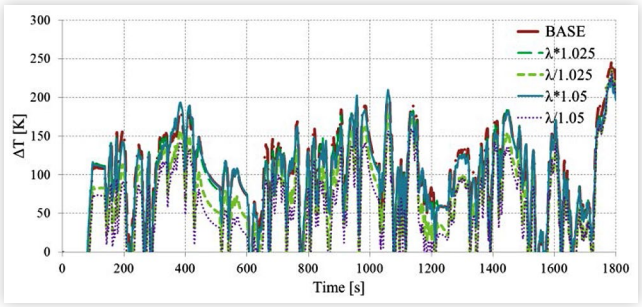

FIGURE 12 Cumulative emissions for varying λ, CO (a), THC (b), NO (c).

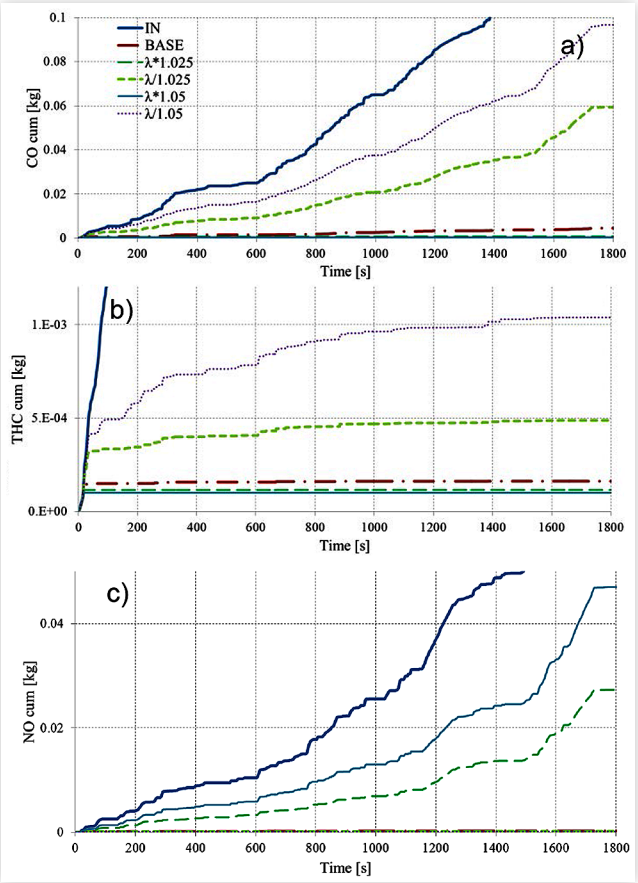

FIGURE 13 CO emission peaks in the time span [650,700]s for different λ (base case (a), λ*1.05 (b) and λ/1.05 (c)).

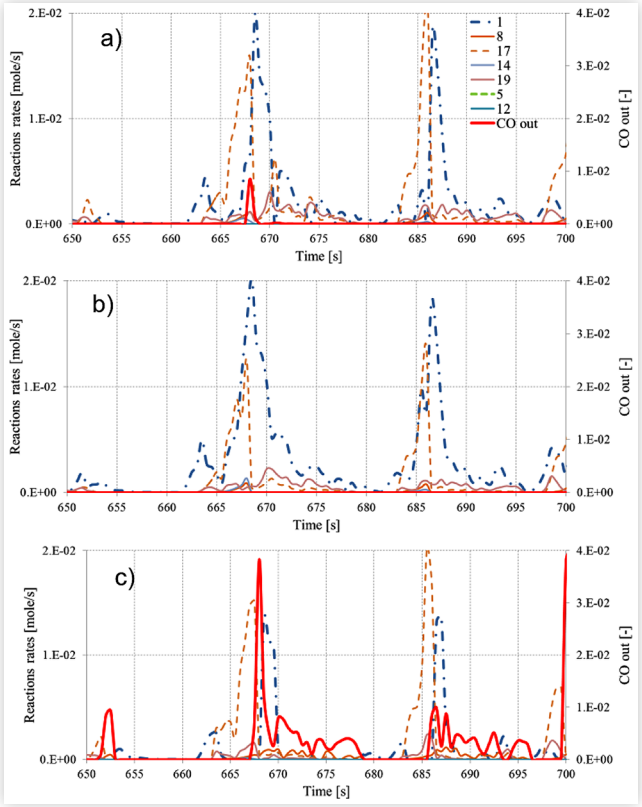

higher λ. For example, a reduction of a factor of 1.05 in λ allows an increase of 0.09% in NO conversion efficiency, while an increase of a factor of 1.05 causes a decrease of 48.7% in NO conversion efficiency.

- Comparing the first 300s and the entire WLTC cycle, the impact of λ is more evident in the first 300s especially for THC. This specie is characterized by a relevant emissions percentage during cold starts. During cold starts, an increase of 1.05 in λ would lead to a reduction of 3% in cumulative emissions, while a reduction of 1.05 in λ would lead to an increase in emission of almost 60% (only 4% for the entire cycle).

Although the time characteristics remain the same, however simulations show that varying λ has an impact on reactions mechanisms. For instance, CO peak happening around 670s described in Fig. 4 has been analyzed for three different λ in Fig. 13. Fig. 13a reports the base case, Fig. 13b reports results with λ*1.05, and Fig. 13c with λ/1.05. The higher λ allows to convert all CO, while the lower λ causes higher and more CO emissions. For a deeper analysis, Fig. 14 compares the same three cases of Fig. 13 in terms of (14a) reaction rate of direct CO oxidation, (14b) reaction rate of CO with surface ceria, (14c) surface CeO_2 flux (14d) and O_{2in} concentration (14e). The effects of varying λ are evident especially on direct oxidation, while weaker on surface ceria reactions. This means that CO depletion is mainly due to direct oxidation.

Effects of varying λ on NO are different with respect to CO and THC. NO emissions increase with increasing λ (in cumulative quantities in Fig. 12c). In fact, reaction rates of NO with CO and surface Ce_2O_3 reduce with increasing λ. This is clear from Fig. 15 where the NO peaks happening in the time range [590,690]s (same time span discussed in Fig. 6 and 7) are described for three different λ concentrations. However, this analysis is valid along the entire WLTC cycle. Fig. 15a reports the NO peak, Fig. 15b reports the rate of NO reduction with CO, while Fig. 15c reports the rate of reaction of NO with surface ceria, for the same three different λ considered in Fig. 14.

Higher λ increases NO peaks both in number and in value. In fact, higher λ implies higher direct oxidation rate of CO, thus less CO available for NO reduction (Fig. 15b). There are instead no evident changes on the reaction rate of surface CeO_2 with NO (Fig. 15c).

Effects of Different PGM Content

The highest contribution to the catalytic converter price is represented by the PGM loading, the material responsible for the catalysis. Interesting is thus to find an optimal PGM content, sufficient to make reactions happening, by minimizing the overall price. In this section the effects of varying PGM in the washcoat have been investigated.

FIGURE 14 Analysis of reaction mechanism related to CO peak in time [650-700]s for varying λ. Description of CO concentrations (a), CO direct oxidation reaction rate (b), surface ceria reactions (c), surface ceria flux (d) and O_{2in} concentrations (e).

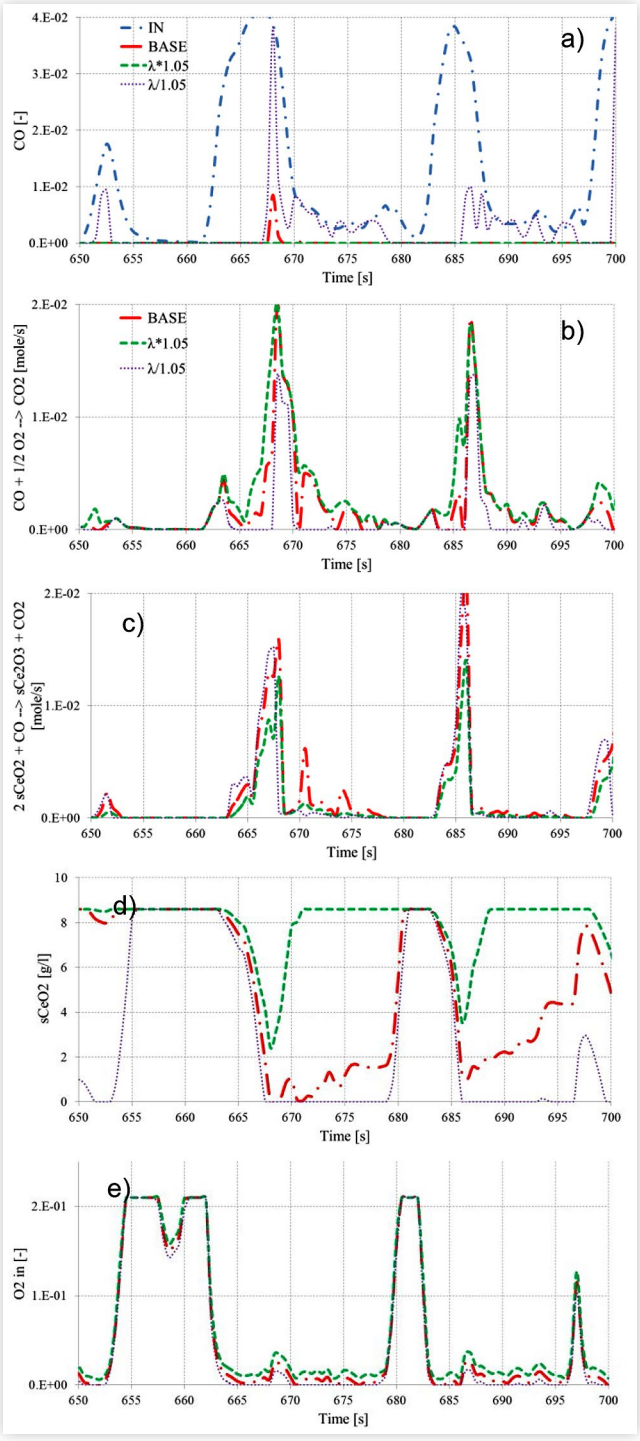

Keeping constant the amount of waschcoat, only the fraction of precious metals has been decreased to 50% and to 20%. Results are reported in terms of cumulative emissions of CO, THC and NO in Fig. 16 and corresponding cumulative efficiencies have been reported in Table 6, both considering the entire WLTC cycle and only in the first 300s. On the whole,

FIGURE 15 Analysis of main reaction mechanisms related to NO peak in time [590-690]s for varying λ. Description of NO concentrations (a), NO reduction rate with CO (b), surface ceria reaction rate (c).

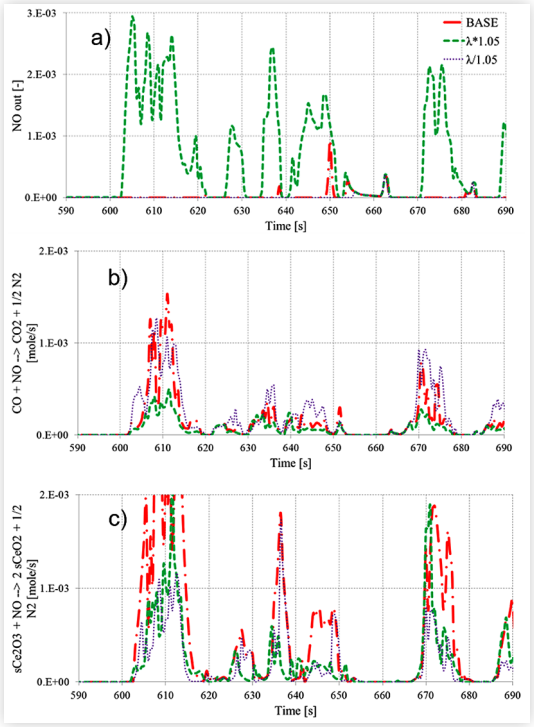

FIGURE 16 Cumulative emissions of CO (a), THC (b) and NO (c) for varying PGM content within the washcoat of the catalytic converter.

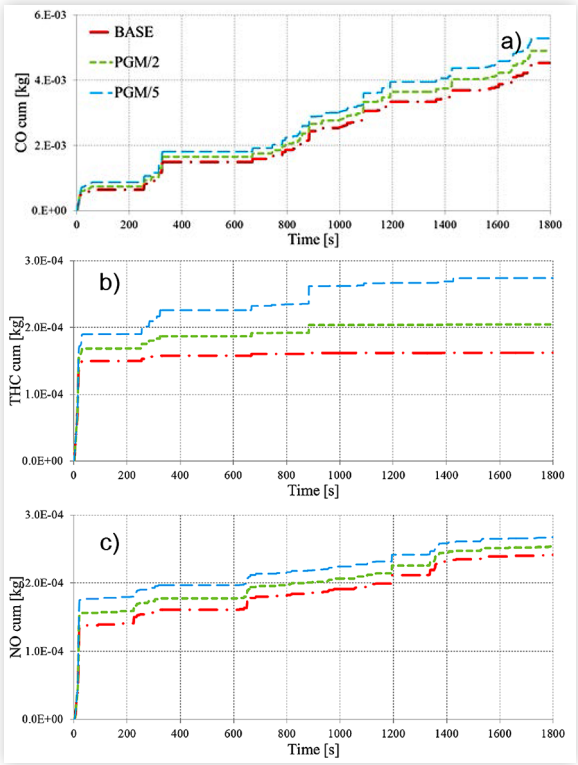

the catalytic converter behavior remains almost the same and emissions are still combination of cold start emissions and discrete break through events. The time properties remain the same, but, according to predictions, emissions slightly increase with decreasing PGM. With 50% less PGM, conversion efficiency decreases of 0.3% and 0.2% respectively for CO and THC, while with only 20% of PGM, conversion decreases 0.5% in both CO and THC. NO reduction remains very high and does not vary significantly. The impact of PGM is stronger on cold starts emissions. In fact, during the first 300s of the cycle, 50% less PGM causes a decrease of 0.7% in CO and 0.8% in THC conversions, while only 20% of the initial PGM causes a reduction of 1.5% and of 1.7% in CO and THC conversion efficiencies.

In addition to overall cumulative emissions, PGM content has an impact also on reaction mechanisms, especially during cold starts. Fig. 17 describes CO peaks during the first 120s for the three different PGM content. Fig. 17a describes CO concentration, Fig. 17b the direct oxidation rate and Fig. 17c the rates of reaction of CO with surface ceria. Lower PGM implies lower mass, thus a faster heat up in the first 20s. With lower PGM the light off temperature is reached before and the emissions reveal to be slightly lower. Instead, after the first 20s, lower PGM implies higher CO emissions. Direct oxidation rate decreases and the mechanism of ceria starts before. This is the reason why in Fig. 17c lower PGM implies higher rate of reactions of CO with surface ceria. The same considerations can be applied to Fig. 18. The interval time [250,300]s is considered. Fig. 18a describes C_3H_6 instantaneous emissions, Fig. 18b the direct oxidation and Fig. 18c the rate of C_3H_6 reacting with surface ceria. Lower PGM implies higher emissions, decreases direct oxidations, while increases surface ceria reactions.

In the same way, Fig 19 describes the effects of different PGM on NO peaks in the time range [620,690]s. Fig. 19a describes NO instantaneous emissions, Fig. 19b the CO reduction and Fig. 19c the reaction rate of NO with surface ceria. NO conversion remains very high and the PGM influence is small. It is clear however that NO reduction with CO is slightly reduced by lower PGM, while surface ceria reactions are facilitated.

FIGURE 17 Analysis of CO main reaction mechanisms in time [0-60]s with different PGM contents. Description of CO concentrations (a), direct oxidation rate of CO (b), surface ceria reaction rate (c).

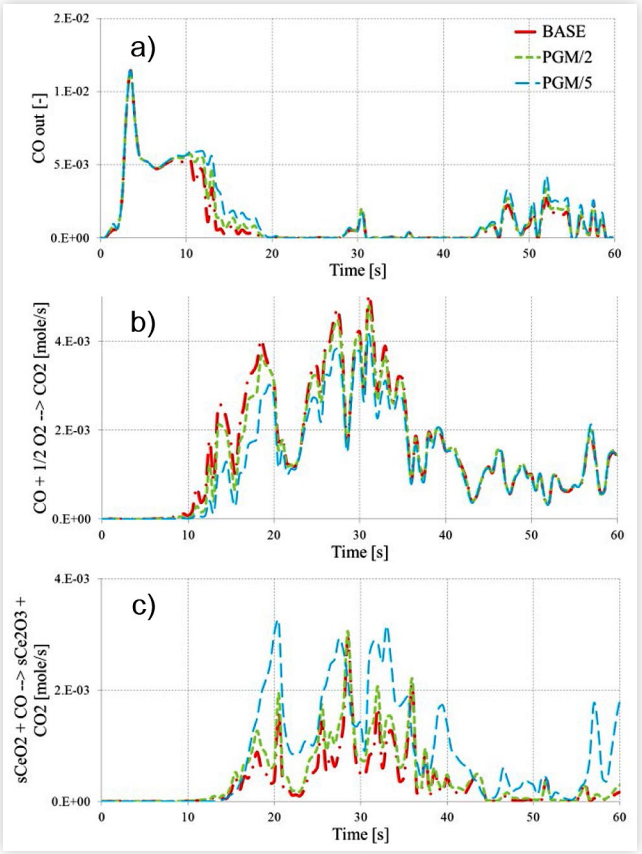

FIGURE 18 Analysis of THC main reaction mechanisms in time [250-300]s with different PGM contents. Description of THC instantaneous concentrations (a), direct oxidation rate (b), surface ceria reaction rate (c).

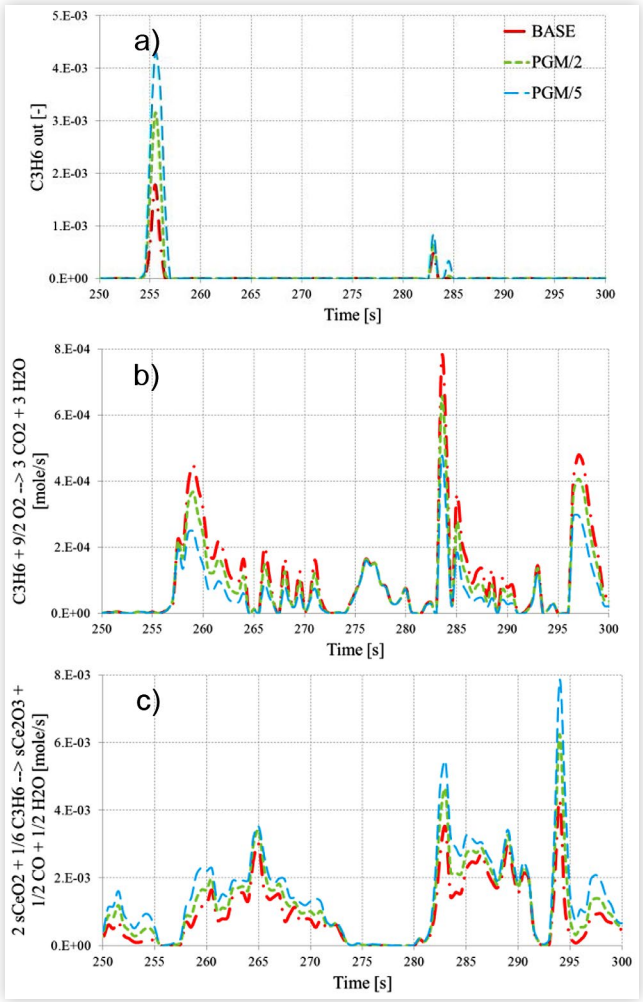

© 2019 SAE International and © 2019 SAE Naples Section. All Rights Reserved.
© 2019 SAE International and © 2019 SAE Naples Section. All Rights Reserved.

FIGURE 19 Analysis of NO main reaction mechanisms in time [620-690]s with different PGM contents. Description of NO concentrations (a), rate of reduction with CO (b), surface ceria reaction rate (c).

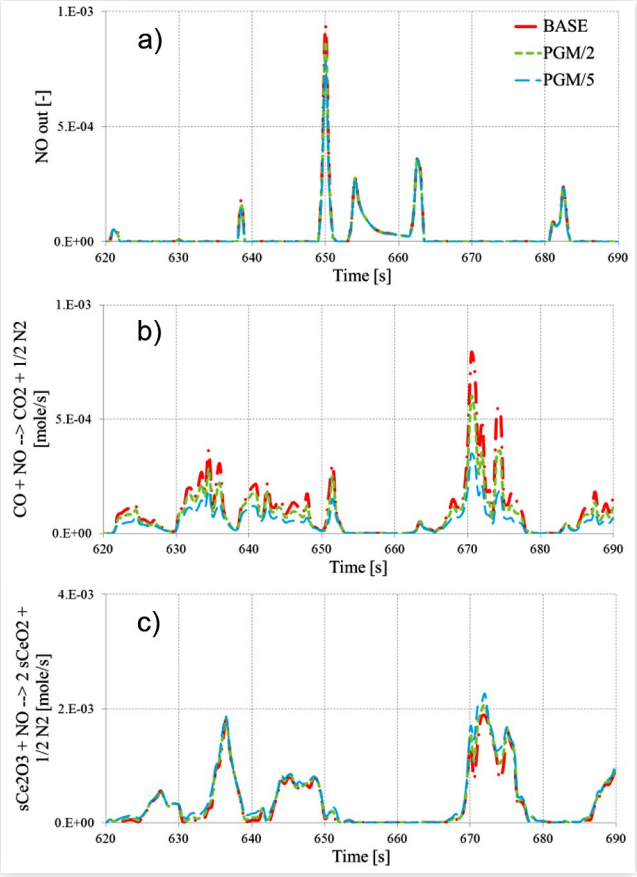

TABLE 6 Cumulative efficiency of CO, THC and NO with different PGM content.

	η_{CO} [%]	η_{THC} [%]	η_{NO} [%]	η_{COcc} [%]	η_{THCcc} [%]	η_{NOcc} [%]
BASE	96.9	99.3	99.8	94.6	95.1	98.0
PGM/2	96.6	99.1	99.7	93.9	94.3	97.8
PGM/5	96.3	98.7	99.7	93.1	93.4	97.6

Conclusions

In the present work, a Gasoline TWC model is implemented in the environment of Axicat, a dedicated application developed by Axisuite. The authors want to offer a detailed analysis of the reaction mechanisms involved in a WLTC cycle of a Euro6 gasoline light duty vehicle within an acceptable computational effort. The model uses a reaction scheme based on 19 brutto reactions (Direct oxidation and reduction, selective catalytic reductions with CO, C_3H_6 and H_2, steam reforming, water-gas shift and bulk ceria as well as surface ceria reactions) described with Langmuir-Hinshelwood expressions. The model is tuned through experiments of a Euro6 gasoline light duty vehicle at the chassis dynamometer during several real driving cycles. Precisely, the reaction parameters in Langmuir-Hinshelwood have been tuned. Moreover, the effects of varying λ and PGM in the waschcoat have been analysed. The final goal is to understand the chemistry inside a TWC, including ceria mechanisms, and to develop an optimized catalytic converter configuration both in terms of geometry and in washcoat compositions. First of all, the following insights can be summarized:

- Based on the reactions taken into account, the real vehicle emissions of a WLTC cycle can be predicted with good accuracy both in terms of time history and in terms of final cumulative emissions values.
- Cycle emissions comprise mainly the cold start contribution as well as discrete emission break-through events during transients. This is evident especially in simulations, less in experiments where the results are made smoother by the measurement setup.

Considering warm conditions, the analysis of the involved reaction mechanisms has shown that:

- The main chemical reactions depleting CO and THC are direct oxidation and surface ceria reactions.
- CO and THC peaks are discrete and simultaneous.
- Each discrete peak of CO and THC is characterized by the same phenomena: following a fuel cutoff phase, during the reacceleration, a rich combustion phase in the engine occurs and O_2 is consumed, thus halting direct oxidation. Thereafter ceria reactions are responsible for the oxidation till CeO_2 cites are depleted. At this point the peak occurs.
- Different mechanisms are leading to NO peaks, which are associated to phases with high oxygen amounts in the catalyst: the main mechanisms are reduction with CO, surface ceria reactions and with H_2. At high NO concentrations coming from the engine, reaction rates are not strong enough for completing reduction.

Of great interest is the investigation of reaction mechanisms during cold starts. Conventionally, the period [0,300] s has been considered. Simulation results have shown that:

- Within the first 20s, no reactions take place due to low temperature, thus catalyst inactivity.
- CO, THC and NO peaks are simultaneous.
- CO and THC peaks are due to lack of O_2 and surface ceria, similarly to the phenomena characteristic in the warm phase.
- NO peaks are due to lack of CO available and surface ceria.

Based on the crucial role played by O_2 in the reaction mechanisms, the effects of varying λ content in the engine and thus in the exhaust gas have been investigated.

- Higher λ reduces CO and THC emissions, due to the fact that direct oxidation rates increase.

- Higher λ content increases NO emissions. In fact, there is less CO available for NO reductions.

The effect of reducing PGM content is also studied, since the most relevant source for cost for the TWC is represented by the PGM loading. It is noticed that:

- Lower PGM loading increases CO and THC cumulative emissions, while the impact on NO emissions is negligible.
- The effect of PGM amount is mainly evident during cold start.
- The reaction mechanisms responsible for the reduction of all the pollutant in question remain similar; however, in general, there is a reduction in direct oxidation, while an increase in ceria reactions rates.

Acknowledgements

The authors gratefully acknowledge the Swiss federal Office for Environment for the project "Modellierung und Validierung des Katalysatorverhaltens bei Kaltstart und im Gesamtzyklus", contract no 15.0002.PJ / S122-1359, for the financial support.

Nomenclature

CUM - Cumulative

in - at inlet of the catalytic converter

out - at outlet of the catalytic converter

λ - fuel air equivalence ratio [-]

Tg in - Inlet gas temperature [K]

$\mathbf{A_i}$ - reaction rate constant [mol/(m^3 s)]

$\mathbf{E_i}$ - reaction activation energy (J/mol)

t - time (s)

T - temperature (K)

THC - total unburnt hydrocarbons

$\mathbf{G_{Ri}}$ - inhibition coefficient (K)

$\mathbf{C_{p,i,s}}$ - reactant concentration (mol/mol)

$\mathbf{R_i}$ - reaction rate (mol/s)

OSC - oxygen storage capacity (mol/m^3)

PGM - Platinum Group Metals

V - vehicle velocity [km/h]

References

1. Omoto, H., Kobayashi, T., Ishikawa, K., and Yamada, T., "Catalyst Design for Meeting Stringent LEV-2 NO_x Regulation," SAE Technical Paper 2002-01-0348, 2002, doi:10.4271/2002-01-0348.
2. Truex, T., Golden, S. J., Polli, A. D., Hawthorne, R. et al., "Advanced Low Platinum Group Metal Three-Way Catalyst for LEV-II and ULEV-II Compliance," SAE Technical Paper 2002-01-0344, 2002, doi:10.4271/2002-01-0344.
3. Twigg, M. V., Collins, N. R., Morris, D., Cooper, J. A. et al., "High Temperature Durable Three-Way Catalysts to Meet European Stage IV Emission Requirements," SAE Technical Paper 2002-01-0351, 2002, doi:10.4271/2002-01-0351.
4. Tsinoglou, D. N., Dimopoulos Eggenschwiler, P., Thurnheer, T., and Hofer, P., "A Simplified Model for Natural-Gas Vehicle Catalysts with Honeycomb and Foam Substrates," *Proceedings of the Institution of Mechanical Engineers, Part D: Journal of Automobile Engineering* 223:819, 2009, doi:10.1243/09544070JAUTO1095.
5. Chatterjee, D., Deutschmann, O., and Warnatz, J., "Detailed Surface Reaction Mechanism in a Three-Way Catalyst," *Faraday Discuss.* 119:371-384, 2001.
6. Voltz, S. E., Morgan, C. R., Liederman, D., and Jacob, S. M., *Ind. Eng. Chem. Prod. Res. Dev.*, 12:294, 1973.
7. Oh, S. and Cavendish, J., "Transients of Monolithic Catalytic Converters: Response to Step Changes in Feedstream Temperature as Related to Controlling Automobile Emissions," *Ind. Eng. Chem. Prod. Res. Dev.*, 21:29-37, 1982.
8. Koltsakis, G. C., Konstantinidis, P. A., and Stamatelos, A. M., "Development and Application Range of Mathematical Models for 3-Way Catalytic Converters," *Appl. Catal. B: Environ.*, 12:161-191, 1997.
9. Tsinoglou, D. N., Koltsakis, G. C., and Peyton Jones, J. C., "Oxygen Storage Modeling in Three-Way Catalytic Converters," *Ind. Eng. Chem. Res.* 41:1152-1165, 2002.
10. Muske, K. R. and Peyton Jones, J. C., "Multi-Objective Model-Based Control for an Automotive Catalyst," *J. Process Control* 16:27-35, 2006.
11. Depcik, C. and Assanis, D., "One-Dimensional Automotive Catalyst Modeling," *Prog. Energy Combust. Sci.* 31(4):308-369, 2005.
12. Papetti, V., Dimopoulos Eggenschwiler, P., Della Torre, A., Lucci, F. et al., "Additive Manufactured Open Cell Polyhedral Structures as Substrates for Automotive Catalysts Int," *J. Heat Mass Transf.* 126:1035-1047, 2018, doi:10.1016/j.ijheatmasstransfer.2018.06.061.
13. Koltsakis, G., Katsaounis, D., Samaras, Z., Naumann, D. et al., "Development of Metal Foam Based Aftertreatment on a Diesel Passenger Car," SAE Technical Paper 2008-01-0619, 2008, doi:10.4271/2008-01-0619.
14. Giani, L., Groppi, G., and Tronconi, E., "Masstransfer Characterization of Metallic Foams as Supports for Structured Catalysts," *Ind. Engng Chem. Res.* 44(14):4993-5002, 2005.
15. Incera Garrido, G., Patkas, F. C., Lang, S., and Kraushaar-Czarnetzki, B., "Mass Transfer and Pressure Drop in Ceramic Foams: A Description for Different Pore Sizes and Porosities," *Chem. Engng Sci.* 63(21):5202-5217, 2008.
16. Papetti, V., Dimopoulos Eggenschwiler, P., Schreiber, D., Reduction of Cold Start Emissions with Microwave Heated Catalytic Converters. in *19th Stuttgart International Symposium on Automotive and Engine Technologies*.

17. Chen, D. K. S. and Cole, C. E., "Numerical Simulation and Experimental Verification of Conversion and Thermal Responses for a Pt/Rh Metal Monolithic Converter," SAE Technical Paper 890798, 1989, doi:10.4271/890798.

18. Gottberg, I., Rydquist, J., Backlund, J., Wallman, S. et al., "New Potential Exhaust Gas Aftertreatment Technologies for "Clean Car" Legislation," SAE Technical Paper 910840, 1986, doi:10.4271/910840.

19. Axisuite, Exothermia.

ISSN 0148-7191